MESOSCOPIC MODELING OF THE RTM PROCESS FOR HOMOGENIZATION

C. Dammann*, R. Mahnken†

*, †Chair of Engineering Mechanics (LTM)
University of Paderborn
Warburger Str. 100, 33098 Paderborn, Germany
*e-mail: dammann@ltm.upb.de
†e-mail: mahnken@ltm.upb.de, web page: http://www.ltm.upb.de/

Key words: Curing, shrinkage, thermal-mechanical-chemical coupling, homogenization, multi-scale modeling, finite elements

Abstract.

Intrinsic hybrids can be manufactured in a modified resin transfer molding (RTM) process for fibre reinforced polymers. Our work concentrates on mesoscopic modeling for temperature-dependent visco-elastic effects accompanied by curing within the RTM process. During hybridization and later thermal loading the periodic mesostructure defined by resin and fibres is taken into account as a representative volume element (RVE) subjected to thermo-mechanical loading. Homogenization leads to results on the less resolved macroscale. In the examples we illustrate the characteristic behavior of the mesoscopic model, such as shrinking due to curing and temperature dependence and simulate the RTM process as well as thermal loading of the cured composite with the finite-element-method.

1 INTRODUCTION

Nowadays, polymeric materials find their applications in carbon- and glass fibre-reinforced epoxy laminates. The production process of polymeric materials is mainly characterised by thermal loading and curing. Here, in the initial uncured state the mixture of resin and curing agent exhibits a viscous liquid behavior allowing no more than hydrostatic pressure. With evolving curing polymer chains form and cross-link to each other such that the viscosity of the liquid resin, its molecular weight and the stiffness increase, see e.g. [1]. The process is highly temperature dependent and influences strongly the mechanical, thermal and chemical properties of the final composite.

In [2] a phenomenological thermo-viscoelastic curing model for finite strain deformations is proposed. The formulation is based on process dependent viscosities.

Furthermore, [3], [4] and [5] formulate ad hoc assumptions for the bulk heat-dilatation coefficient dependent on curing, whereas the bulk shrinking-dilatation coefficient is not dependent on the degree of curing.

A micro-macro strategy suitable for modeling the mechanical response of heterogeneous materials at large deformations and non-linear history dependent material behaviour is presented in [6]. [7] investigates an algorithm for the computation of homogenized stresses by volume averaging and the overall tangent moduli of microstructures undergoing small strains is derived. In [8], the influence of the RVE size on the residual stresses created during the curing process of a continuous fibre-reinforced polymer matrix tow is investigated to calculate the response of woven fibre textile composites. Additionally, mechanical loading for varying RVE size is investigated, not including the effect of curing stresses, or in other words not including the process history.

Our work enhances these investigations, concentrating on the macroscopic anisotropic thermal expansion coefficient including the history of a modfied RTM process. Within a thermodynamic framework we use an additive ternary decomposition of the logarithmic Hencky strain tensor into mechanical, thermal and chemical parts, as in [4]. Based on the concept of stoichiometric mass fractions [9] for resin, curing agent and solidified material the bulk compression modulus as well as the bulk heat- and shrinking dilatation coefficients are derived. An RVE simulating the RTM process is used to determine the macroscopic strains by homogenization. Mesoscopic as well as macroscopic residual strains can be observed for the fully cured material. Based on this foundings, the macroscopic anisotropic thermal extension is determined.

Notations

Square brackets [$\bullet$] are used throughout the paper to denote 'function of' in order to distinguish from mathematical groupings with parenthesis ($\bullet$).

2 A GENERAL FRAMEWORK FOR FIBRE REINFORCED POLYMER CURING

Within the framework of large strain theory $\mathcal{B}_0 \subset \mathcal{R}^3$ in Figure 1.b denotes the periodic mesostructure of a fibre reinforced composite in the reference configuration. It is related to the homogenized macrocontinuum in the reference configuration $\bar{\mathcal{B}}_0 \subset \mathcal{R}^3$, as shown in Figure 1.a. $\mathcal{V}_0$ in Figure 1.c denotes the RVE associated with the structure $\mathcal{B}_0$. The volume $\mathcal{V}_0$ consists of the resin part $\mathcal{B}_{0resin}$ and the fibre part $\mathcal{B}_{0fibre}$, respectively, each regarded as solid constituents. Thus, we consider the decompositions of the RVE and its surface $\mathcal{V}_0 = \mathcal{B}_{0resin} \cup \mathcal{B}_{0fibre}$. We denote by $P_i \subset \mathcal{B}_{0i}$, a spatial point for which either $i = resin$ or $i = fibre$ holds. Its material counterpart at time t in the current configuration of the mesostructure $\mathcal{B}_i$, $i = resin$, $fibre$ in the space-time-domain $\mathcal{B}_0 \times \,] - \infty, T[$ is denoted by p_i, $i = resin$, $fibre$, where T is the total time of interest.
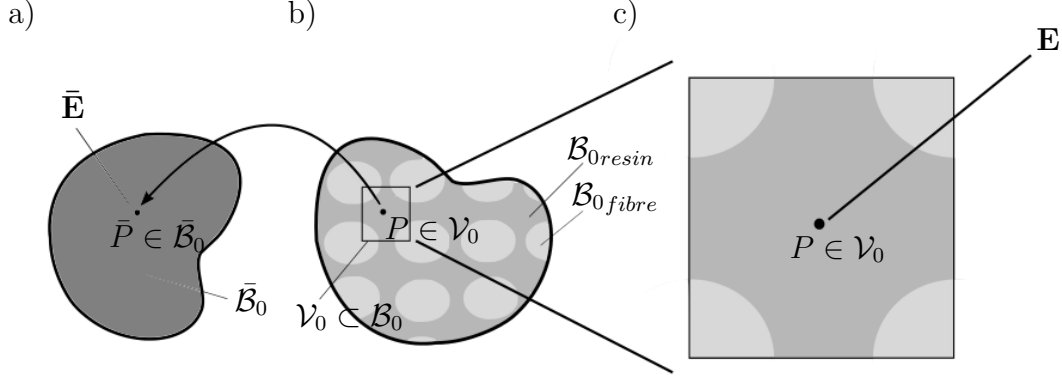
a)　　　　　　　　b)　　　　　　　　c)

Figure 1: Macrocontinuum with a mesostructure: a) Homogenous macrocontinuum $\bar{\mathcal{B}}_0$ and strain $\bar{\mathbf{E}}$ at point $\bar{P}$, b) periodic mesostructure $\mathcal{B}_0$ and RVE $\mathcal{V}_0$, c) RVE with strain $\mathbf{E}$ at point P.

Additionally, the deformation gradient $\mathbf{F}_i$, $i = resin,\ fibre$ is introduced at each material point p_i. It maps line segments $d\mathbf{X}_i$ of the reference configuration $\mathcal{B}_{0i}$ to line segments $d\mathbf{x}_i$ of the current configuration $\mathcal{B}_i$. Additionally, we introduce its Jacobian $J_i = \det \mathbf{F}_i$, mapping a volume element dV_i of the reference configuration $\mathcal{B}_{0i}$ to a volume element dv_i of the current configuration $\mathcal{B}_i$:

$$1.\ \ d\mathbf{x}_i = \mathbf{F}_i \cdot d\mathbf{X}_i, \quad 2.\ \ dv_i = J_i dV_i, \quad i = resin,\ fibre. \tag{1}$$

A key point in constructing a framework of finite plasticity is the definition of the total Hencky strain tensor $\mathbf{E}_i$ in a logarithmic form, see e.g. [10, 11].We assume this strain measure to be a function of the right Cauchy-Green tensor

$$1.\ \mathbf{C}_i = \mathbf{F}_i^t \cdot \mathbf{F}_i, \quad 2.\ \mathbf{E}_i = \frac{1}{2} \ln \mathbf{C}_i, \quad i = resin,\ fibre. \tag{2}$$

The volumetric and deviatoric parts of the Hencky strain tensor are defined as

$$1.\ \ \mathbf{E}_i^{vol} = \frac{1}{3} \mathrm{tr} \mathbf{E}_i\ \mathbf{1}, \quad 2.\ \ \mathbf{E}_i^{dev} = \mathbf{E}_i - \mathbf{E}_i^{vol}, \quad i = resin,\ fibre. \tag{3}$$

3 MESOSCOPIC MODELING

The models for the composite constituents are described in the following subsections 3.1 and 3.2. The resin is modeled as visco-elastic and the fibre is considered as a thermo-linear-elastic solid. For notational benefits, the index $i = resin,\ fibre$ is omitted.

3.1 Modeling of resin: visco-elasticity coupled to curing

Based on the concept of stoichiometric mass fractions as discussed extensively in [9] for resin, curing agent and solidified material the *bulk compression modulus* κ, the *bulk heat-dilatation coefficient* α and the *shrinking dilatation coefficient* β are derived. For subsequent analysis, we assume that α is dependent on the pressure p, the temperature $\theta[t]$ and the *degree of cure* $z[t]$. Additionally we assume that the *bulk curing-dilatation coefficient* β is dependent on the pressure p and the temperature $\theta[t]$.

3.1.1 Mass fractions and the degree of cure

We assume a homogeneous mixture with three constituents resin, curing agent and solidified material at each instant of time t. As a consequence there are neither concentration gradients nor diffusion effects. With the time-dependent variables $dm_r[t], dm_{ca}[t]$ and $dm_{sol}[t]$ for the masses of resin, curing agent and solidified material, respectively, the conservation of mass during the curing reaction requires

$$dm_r[t] + dm_{ca}[t] + dm_{sol}[t] = dm_0 = \text{const}, \tag{4}$$

where the constant dm_0 is the total mass of the mixture [9]. Dividing Eq.(4) by dm_0 and introducing the mass fractions of resin, curing agent and solid

$$\zeta_r[t] = \frac{dm_r[t]}{dm_0}, \quad \zeta_{ca}[t] = \frac{dm_{ca}[t]}{dm_0}, \quad \zeta_{sol}[t] = \frac{dm_{sol}[t]}{dm_0}, \tag{5}$$

we obtain the balance relation

$$\zeta_r[t] + \zeta_{ca}[t] + \zeta_{sol}[t] = 1. \tag{6}$$

As explained in [9] the number of variables can be reduced by taking into account the stoichiometry of the mixture. To this end the *degree of cure* $0 \leq z[t] \leq 1$ is introduced, see also [1], such that the mass fractions of the three components of the mixture are written in the form

$$
\begin{aligned}
1. \ \zeta_r[t] &= n(1 - z[t]) \\
2. \ \zeta_{ca}[t] &= (1 - n)(1 - z[t]) \\
3. \ \zeta_{sol}[t] &= z[t].
\end{aligned}
\tag{7}
$$

The initial state with $z[0] = 0$ corresponds to the uncured, viscous mixture with $\zeta_r[0] = n$, $\zeta_{ca}[0] = n - 1$, $\zeta_{sol}[0] = 0$ as initial conditions. Consequently, n and $1 - n$ are the mass fractions of the resin and the curing agent at the beginning of curing, respectively. The final fully cured state at time $t \to \infty$ with $z[\infty] = 1$ corresponds to the solidified material at the end of the reaction, i.e. $\zeta_r[\infty] = \zeta_{ca}[\infty] = 0$ and $\zeta_{sol}[\infty] = 1$.

In the subsequent exposition, occasionally an index $i = r, ca, sol$ referring to resin, curing agent and solidified material will be used. Then, Eq.(6) and the connectivity for all three constituents renders the following balances at each body point $\mathbf{X} \in \mathcal{B}_0$ and for all times $t > -\infty$:

$$1. \ \sum_{i=1}^{3} \zeta_i = 1, \qquad 2. \ \zeta_i \geq 0, \quad i = r, ca, sol. \tag{8}$$

Furthermore, from Eq.(7) we obtain the functional relation

$$\zeta_i = \zeta_i[z], \qquad i = r, ca, sol, \tag{9}$$

which means, that the mass phase fractions ζ_i are independent of temperature and deformation.

We also assume, that the mixture for the resin is homogeneous, i.e. all phases are equally distributed. Then, the (bulk) densities ρ_0 and ρ of the mixture with respect to the reference and the current configurations $\mathcal{B}_0$ and $\mathcal{B}$ are respectively defined as

$$1. \quad \varrho_0 = \frac{dm}{dV}, \qquad\qquad 2. \quad \varrho = \frac{dm}{dv}. \tag{10}$$

Here, according to Eq.(1) dv and dV are the volume differentials of the mass differential dm at the reference and the current configurations, respectively.

Within the volume dv, let the ith constituent have its volume dv_i and its mass dm_i, $i = r, ca, sol$. Then, the mass phase fraction ζ_i and the density of the ith constituent are defined by

$$1. \quad \zeta_i = \frac{dm_i}{dm}, \qquad\qquad 2. \quad \rho_i = \frac{dm_i}{dv_i}. \tag{11}$$

The equations (10) and (11) imply the assumption, that the quantities ρ and ρ_i at a body point $P \in \mathcal{B}_0$ are defined by a limit process with volumes contracting to this point. Using Eq.(10), the relation $dv = \sum_{i=1}^{3} dv_i$ as well as Eq.(11.2) and Eq.(11.1) renders the following mixture rule for the inverse of the bulk density ρ

$$\frac{1}{\rho} = \frac{dv}{dm} = \frac{\sum_{i=1}^{3} dv_i}{dm} = \sum_{i=1}^{3} \frac{dm_i}{\rho_i dm} = \sum_{i=1}^{3} \frac{\zeta_i}{\rho_i}. \tag{12}$$

For the subsequent analysis, we assume that the density of each constituent is solely dependent on the pressure p and the temperature, that is

$$\rho_i = \rho_i[p, \theta]. \tag{13}$$

Note, that the functional relations (9) and (13) combined with the mixture rule Eq.(12) imply the functional relation

$$\rho[t] = \rho[p[t], \theta[t], z[t]], \tag{14}$$

i.e. the density change is induced by pressure p, temperature θ and/or by curing z.

3.1.2 Volume changes due to density changes

We assume that the total volume change J in Eq.(1.2) is multiplicatively decomposed into an effective part (induced by pressure p), a thermal part (induced by temperature θ) and a chemical part (induced by curing z as a result of shrinkage due to polymerization), that is

$$J = \frac{dv}{dV} = \frac{\rho_0}{\rho} = J^p \cdot J^\theta \cdot J^z. \tag{15}$$

717

Using the relation (12) and exploiting the functional relation (13), the time derivative of J for the third part in Eq. (15) is expressed as follows:

$$\dot{J} = \frac{d}{dt}\left(\frac{\rho_0}{\rho}\right) = \rho_0\frac{d}{dt}\left(\sum_{i=1}^{3}\frac{\zeta_i}{\rho_i}\right) = -\sum_{i=1}^{3}\rho_0\frac{\zeta_i}{\rho_i^2}\frac{\partial\rho_i}{\partial p}\ \dot{p} - \sum_{i=1}^{3}\rho_0\frac{\zeta_i}{\rho_i^2}\frac{\partial\rho_i}{\partial\theta}\ \dot{\theta} + \sum_{i=1}^{3}\frac{\rho_0}{\rho_i}\frac{\partial\zeta_i}{\partial z}\ \dot{z}. \quad (16)$$

Next we define the isothermal compressibility κ, the (uni-directional) bulk heat-dilatation coefficient α and the (uni-directional) bulk curing-dilatation coefficient β:

$$
\begin{array}{llll}
1. & \kappa[p,\theta,z] = \sum_{i=1}^{3}\kappa_i[p,\theta]\zeta_i, & \text{where} \quad 2. & \kappa_i[p,\theta] = \dfrac{\rho_0}{\rho_i^2}\dfrac{\partial\rho_i}{\partial p} \\[3mm]
3. & \alpha[p,\theta,z] = \sum_{i=1}^{3}\alpha_i[p,\theta]\zeta_i, & \text{where} \quad 4. & \alpha_i[p,\theta] = \dfrac{-\rho_0}{3\rho_i^2}\dfrac{\partial\rho_i}{\partial\theta} \\[3mm]
5. & \beta[p,\theta] = \sum_{i=1}^{3}\beta_i[p,\theta]\dfrac{\partial\zeta_i}{\partial z}, & \text{where} \quad 6. & \beta_i[p,\theta] = \dfrac{\rho_0}{3\rho_i}.
\end{array}
\quad (17)
$$

For the mass fractions of the three constituents in Eq.(7), the bulk heat-dilatation coefficient in Eq.(17.3) is

$$\alpha[p,\theta,z] = \alpha_r[p,\theta]\ n(1-z) + \alpha_{ca}[p,\theta]\ (1-n)(1-z) + \alpha_{sol}[p,\theta]\ z, \quad (18)$$

where $\alpha_r[p,\theta]$, $\alpha_{ca}[p,\theta]$ and $\alpha_{sol}[p,\theta]$ are defined according to Eq.(17.4). In general, for increasing temperature θ the densities ρ_i decrease, i.e. $\partial\rho_i/\partial\theta$ is negative, such that $\alpha_i[p,\theta], i = r,\ ca,\ sol$ are positive. The bulk curing-dilatation coefficient β in Eq.(17.5) is

$$\beta[p,\theta] = -n\beta_r[p,\theta] - (1-n)\beta_{ca}[p,\theta] + \beta_{sol}[p,\theta], \quad (19)$$

where $\beta_r[p,\theta]$, $\beta_{ca}[p,\theta]$ and $\beta_{sol}[p,\theta]$ are defined according to Eq.(17.6). In general we have $\rho_{sol} > \rho_r$ and $\rho_{sol} > \rho_{ca}$, such that $\beta[p,\theta]$ is negative.

3.1.3 Strains and stresses

The thermal and the curing strains

$$
\begin{array}{lll}
1. & \mathbf{E}_{th} = \int_{s=-\infty}^{t}\mathbf{E}_{th} = \int_{s=-\infty}^{t}\alpha[s]\dfrac{d\theta}{ds}ds\mathbf{1} \\[4mm]
2. & \mathbf{E}_{cur} = \int_{s=-\infty}^{t}\beta[s]\dfrac{dz}{ds}ds\mathbf{1},
\end{array}
\quad (20)
$$

are governed by α and β which are in accordance with Eqn.(17.3,17.5). In [4], the effective strain tensor is obtained with $\mathbf{E}$ from Eq.(2.2):

$$\mathbf{E}^p = \mathbf{E} - \mathbf{E}_{th} - \mathbf{E}_{cur}. \quad (21)$$

Additionally, we define the Hill-stress tensor $\mathbf{T} = \mathbf{T}_{vol} + \mathbf{T}_{dev}$ with volumetric and deviatoric parts

$$
\begin{aligned}
1. \quad \mathbf{T}_{vol} &= \int_{s=-\infty}^{t} \frac{1}{\kappa[s,t]} \frac{d}{ds} \mathrm{tr}[\mathbf{E}^p[s]] \; \mathbf{1} \; ds \\
2. \quad \mathbf{T}_{dev} &= \int_{s=-\infty}^{t} 2G[s,t] \frac{d}{ds} \mathbf{E}^{dev}[s] ds.
\end{aligned}
\tag{22}
$$

The compressibility κ in Eq.(22.1) is obtained in the same fashion as α in Eq.(18), and G Eq.(22.2) is the shear modulus, in detail described in [4].

3.2 Modeling of fibre: thermo-linear-elasticity

The fibre is considered as a thermo-linear-elastic solid. Consequently it can be modeled as a special case with the equations of subsection 3.1. For example, taking into account Eq.(21) with $\zeta_{sol} = 1$ and $\mathbf{E}_{cur} = 0$ in Eq.(20.2), Eq.(21) reduces to $\mathbf{E}^p = \mathbf{E} - \mathbf{E}_{th}$.

4 MESO TO MACRO TRANSITION

The mesostructure variables are related to the homogenized macrocontinuum $\bar{\mathcal{B}}_0 \subset \mathcal{R}^3$ by use of the Volume Averaging Theorem, as formulated in [12]. Based on the decomposition $\mathcal{V}_0 = \mathcal{B}_{0resin} \cup \mathcal{B}_{0fibre}$ in Section 2 we define the overall macro-strain $\bar{\mathbf{E}}(t)$ of the mesostructure $\mathcal{B}_0$ in relation to the strains from Eq.(2.2) as well as the general homogenization operator $\bar{\bullet}$ by

$$
1. \quad \bar{\mathbf{E}} = \frac{1}{|\mathcal{V}_0|} \int_{\mathcal{V}_0} \mathbf{E} dV, \qquad 2. \quad \bar{\bullet} = \frac{1}{|\mathcal{V}_0|} \int_{\mathcal{V}_0} \bullet dV.
\tag{23}
$$

5 NUMERICAL SIMULATION

In this section an RVE is simulated in two loading sequences. The first sequence simulates the RTM process. This leads to residual strains on the mesoscale. Macroscopic strains are determined by homogenization. In the second sequence, based on the process history of the fully cured composite from sequence one, the *macroscopic anisotropic thermal expansion coefficient* is determined.

5.1 Thermal-mechanical-chemical coupling in an RVE during hybridization

In this example some features on the coupling of temperature, curing and visco-elasticity of the model proposed in Section 3 are illustrated for a mesoscopic problem and its homogenized macroscopic answer occuring in the RTM process. To model the three dimensional RVE shown in Figure 2 and representing the composite material on the mesoscale, stiff fibres (bright) are embedded in a soft resin matrix (dark), thus defining $\mathcal{B}_{0fibre}$ and $\mathcal{B}_{0resin}$. The cube-shaped RVE has a fibre-volume-fraction of 19.6 %. The
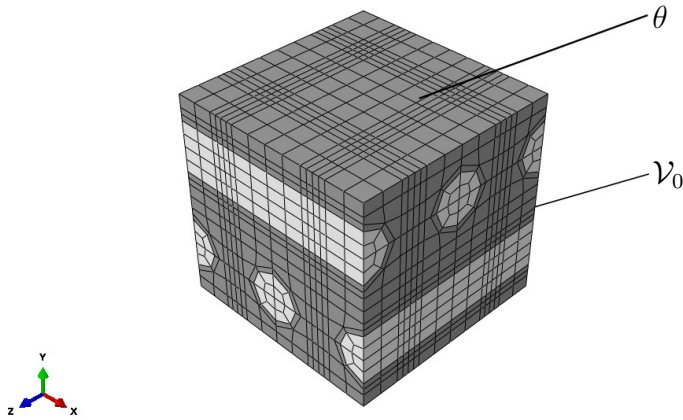
Figure 2: Statically determined RVE $\mathcal{V}_0$: Geometry, FE-discretization and thermal loading θ.

fibres are assumed thermo-elastic, while the matrix material is modeled visco-elastic, see Section 3. Fictive material parameters are chosen. The boundary conditions for the RVE are statically determined to allow thermal expansion, or shrinkage, respectively. Since temperature gradients occuring in the RVE are neglected, the RTM process is assumed to be a pure homogenous thermal loading θ of the RVE denoted as HEAT, CURE and COOL in Figure 2. In the first phase the temperature is increased with constant rate from the initial value $\theta = 25\ °C$ up to $\theta = 120\ °C$. During the second phase, the temperature is kept fixed. In the third phase the temperature is decreased at constant rate to the initial value of $\theta = 25\ °C$.
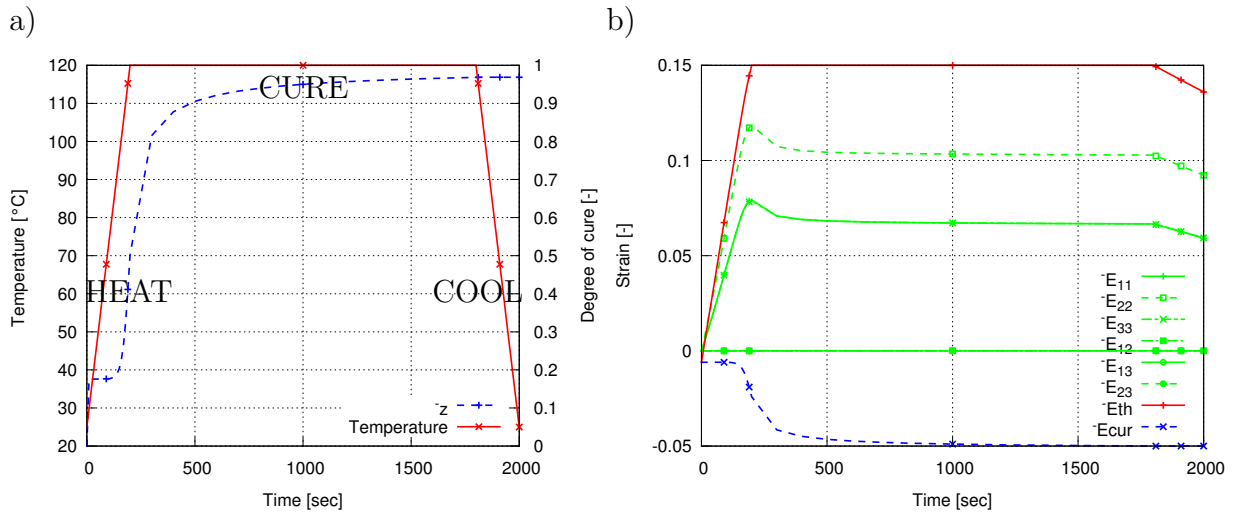

Figure 3: RVE during the RTM process: a) Thermal loading and homogenized degree of cure vs. time, b) components of homogenized strain tensor $\bar{\mathbf{E}}$ and homogenized strains $\bar{\mathbf{E}}_{th}$ and $\bar{\mathbf{E}}_{cur}$ vs. time.
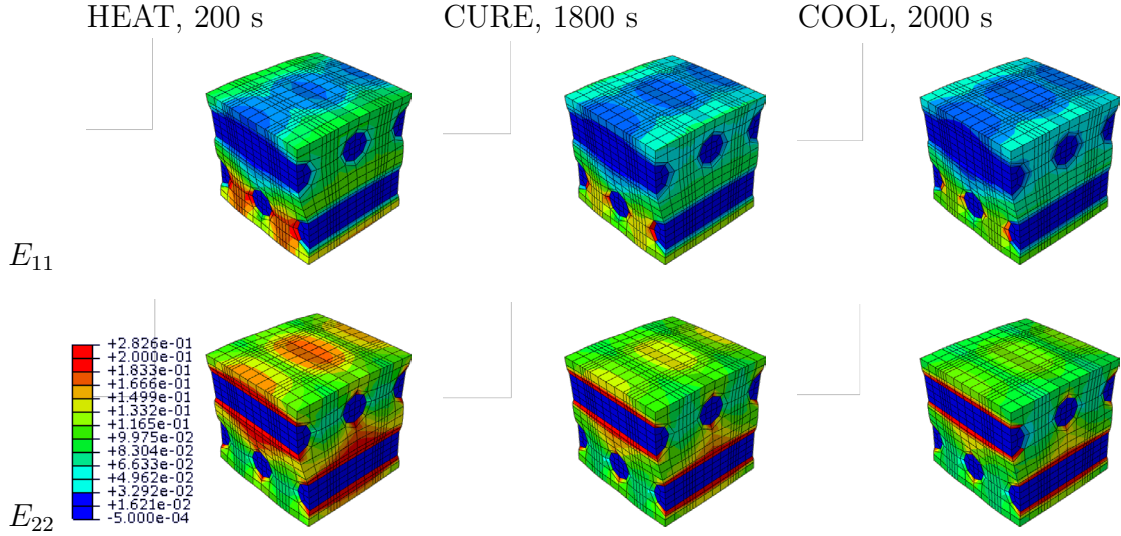
Figure 4: RVE during the RTM process: Contourplots showing strains E_{11} and E_{22} during the three phases of the loading program in Figure 3.a

As mesoscopic strains show symmetries for the x- and z-direction, it is sufficient showing the contourplots in Figure 4 only for the unsymmetric x- and y-directions. The strain contourplots offer residual strains as a remaining strain state for the fully cured composite at the end of phase COOL. This is due to the change of the thermal-expansion coefficient as a result of curing, see Eqn.(18,20.1).

In Figure 3.a-b we summarize some relevant macroscopic quantities resulting from the mechanical-thermal-chemical coupling. The influence of curing and temperature on the homogenized total strains $\bar{\mathbf{E}}$ Eq. (23.1) can be observed. The strains offer a macroscopic orthotropic deformation behavior with a symmetry in x- and z-direction and residual strains at the end of phase COOL. Applying Eq. (23.2), homogenization leads to results for the degree of cure $\bar{z}$ as well as for the uniaxial thermal and shrinking strains $\bar{\mathbf{E}}_{th}$ and $\bar{\mathbf{E}}_{cur}$ shown in Figure 3.a-b. The reason for an initial value for the homogenized degree of cure $\bar{z}_0 > 0$ is that, in contrast to the resin, the fibres initial condition on the mesoscale is $z_0 = 1$. We want to remark, that during the COOL phase linear strain behavior can be observed in Figure 3.b because curing is almost completed at 1600 s. In contrast, in the preceding phases curing governs nonlinear strains.

5.2   Macroscopic thermal expansion coefficient of the fully cured composite

The aim of this example is the determination of the macroscopic thermal expansion coefficient. Thus, the fully cured composite offers a strain state related to residual strains, as shown in Section 5.2. The subsequent loading program shown in Figure 5.a is divided into two phases HOLD and HEAT2 following the three phases in Section 5.2. During the fourth phase the temperature is kept fixed. In the fifth phase the temperature is increased by $\Delta\theta = 1\,°C$. The motivation for the HOLD phase is found in relaxation of strains of
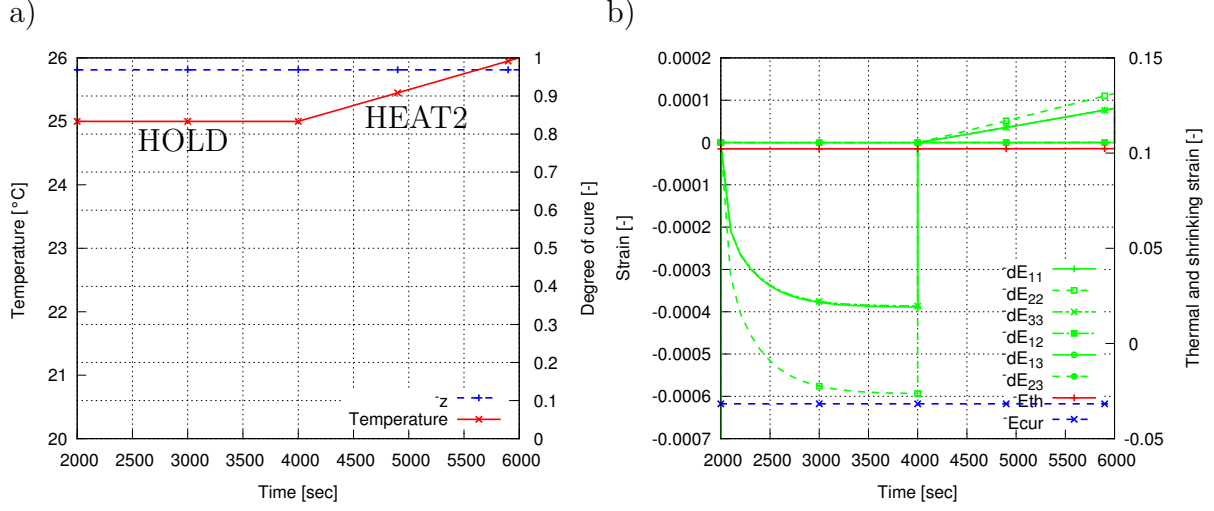
a)

b)

Figure 5: Thermal loading of an RVE: a) Thermal loading and homogenized degree of cure vs. time, b) tensor of homogenized strain increment per phase $\Delta\bar{\mathbf{E}}$ and homogenized strains $\bar{\mathbf{E}}_{th}$ and $\bar{\mathbf{E}}_{cur}$ vs. time.

the visco-elastic material on the mesoscale. To observe this small effect, the mesoscopic strain state at every material point of the mesoscale beyond the COOL phase is divided from the mesoscopic strain state beyond the HOLD phase, resulting in the incremental strains on the mesoscale. Homogenization then leads to

$$\Delta\bar{\mathbf{E}}_{\text{HOLD}} = \bar{\mathbf{E}}_{\text{HOLD}} - \bar{\mathbf{E}}_{\text{COOL}}. \tag{24}$$

$\bar{\mathbf{E}}_{\text{HOLD}}$ and $\bar{\mathbf{E}}_{\text{COOL}}$ are quantities obtained by use of Eq.(23.1) at times $t = 4000$ s and $t = 2000$ s, respectively. As the strain increments $\Delta\bar{\mathbf{E}}$ show asymptotic behavior beyond 3500 s, the HEAT2 phase is started at $t = 4000$ s. Due to very slow heating and small temperatur variation of $\Delta\theta = 1\,°C$ we exclude viscoelastic effects. Thus, the homogenized strain increment $\Delta\bar{\mathbf{E}}$ is directly related to the *anisotropic macroscopic thermal expansion coefficients*

$$\Delta\bar{\mathbf{E}}_{\text{HEAT2}} = \bar{\mathbf{E}}_{\text{HEAT2}} - \bar{\mathbf{E}}_{\text{HOLD}} = \bar{\alpha}. \tag{25}$$

The coefficients of $\bar{\alpha}$ can directly be obtained from Figure 5.b as

$$\bar{\alpha}^T = [8.09 \cdot 10^{-05}, 1.16 \cdot 10^{-04}, 8.02 \cdot 10^{-05}, 1.84 \cdot 10^{-08}, -1.38 \cdot 10^{-11}, 1.86 \cdot 10^{-08}]. \tag{26}$$

As expected, they show orthotropic behavior for the x- and z- components and, except numerical inexactness, shear components xy, xz, $zy = 0$. Thus, the strains due to the HEAT2 phase are very small. Contourplots for the HEAT2 phase displaying strain increments on the mesoscale are illustrated in Figure 6. We want to remark, that the displayed strains $\Delta\mathbf{E}$ are therefore residual strain free, in contrast to those of Figure 4.
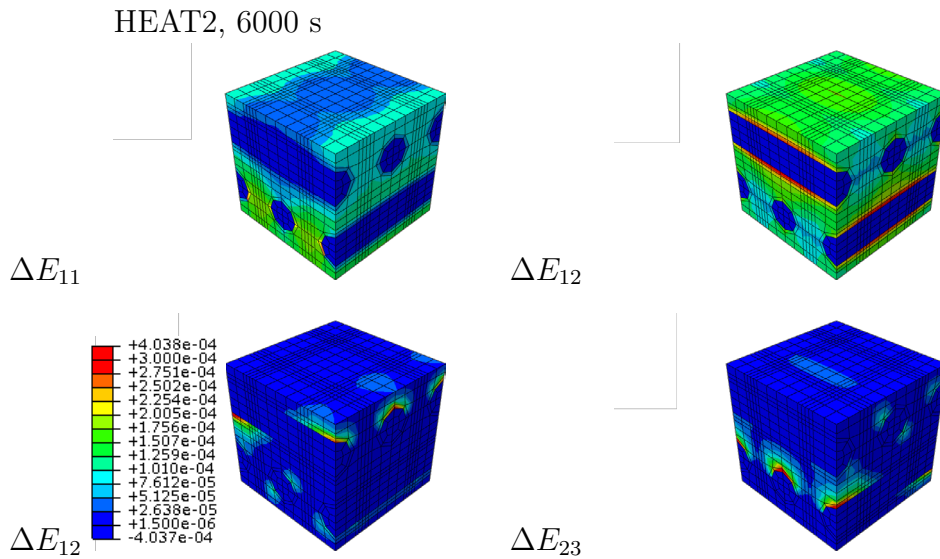
Figure 6: Thermal loading of the RVE: Contourplots showing strain increments ΔE_{11}, ΔE_{22}, ΔE_{12} and ΔE_{23} due to thermal loading HEAT2 following on the HOLD phase according to Figure 5.a

6   CONCLUSIONS

In this paper, we have developed a mesoscopic model for temperature-dependent visco-elastic effects accompanied by curing of fibre reinforced composites, which are important phenomena in production processes. The logarithmic Hencky strain tensor constitutes the basis for the large strain formulation and is additively decomposed into a mechanical, a thermal and a chemical part for the resin as for the fibre. Based on the concept of stoichiometric mass fractions for resin, curing agent and solidified material the bulk heat- and shrinking dilatation coefficients as well as a linear dependence with respect to the degree of curing for the compressibility are derived. The meso to macro transition is treated by use of the Volume Averaging Theorem. In the examples we illustrate the anisotropic shrinking and thermal expansion due to curing as well as temperature dependence. The hybridization process as a modified RTM process is simulated with the finite-element-method for an RVE. Residual process dependent strain states are observed on the mesoscopic as well as on the macroscopic scale for the fully cured composite, which effect later use. Based on the process history, the macroscopic thermal expansion coefficient is determined by further thermal loading of the fully cured RVE. The coefficient mainly shows thermo-elastic orthotropic deformation behavior.

Concerning further extensions, taking a Navier-Stokes equation for the liquid phase of the forming process into account is an area of future research work in the field of fluid-structure interaction with phase transitions.

ACKNOWLEDGEMENT

REFERENCES

[1] Kiasat, M. *Curing shrinkage and residual stresses in viscoelastic thermosetting resins and composites.* PhD Thesis, TU Delft, Netherlands (2000).

[2] Hossain, M., Possart, G., Steinmann, P. A finite strain framework for the simulation of polymer curing. *Comput. Mech.* (2009) **44**:621–630.

[3] Ruiz, E., Trochu, F. Thermomechanical properties during cure of glass-polyester RTM composites: elastic and viscoelastic modeling. *J. Compos. Mater.* (2005) **39**:881–916.

[4] Mahnken, R. Thermodynamic consistent modeling of polymer curing coupled to visco-elasticity at large strains. *Int. J. Solids Struct.* (2013) **50**:2003–2021.

[5] Hill, R., Muzumdar, S.V., Lee, L.J. Analysis of Volumetric Changes of Unsaturated Polyester Resins During Curing. *Polym. Eng. Sci.* (1995) **35**(10):852–859.

[6] Kouznetsova, V., Brekelmans, W. A. M., Baaijens, F.P.T. An approach to micro-macro modeling of heterogeneous materials. *Comput. Mech.* (2001) **27**:37–48.

[7] Miehe, C., Koch, A. Computational micro-to-macro transitions of discretized microstructures undergoing small strains- *Arch. Appl. Mech.* (2002) **72**:300–317.

[8] Heinrich,C., Aldridge, M., Wineman, A.S.,Kieffer, J,Waas, A.M. and Shahwan,K. The influence of the representative volume element (RVE) size on the homogenized response of cured fiber composites. *Modell. Simul. Mater. Sci.* (2012) **20**:75007.

[9] Lion, A., Höfer, P. On the phenomenological representation of curing phenomena in contiuum mechanics. *Archive of Mechanics* (2007) **59**:59–89.

[10] Hencky, H. Über die Form des Elastizitätsgesetzes bei ideal elastischen Stoffen. *Zeitschrift für Technische Physik* (1928) **9**:215–220.

[11] Seth, B.R. *Generalized strain measure with application to physical problems.* Reiner, M., Abir, D., Second Order Effects in Elasticity, Plasticity and Fluid Dynamics (1964).

[12] Hill, R. On constitutive macrovariables for heterogeneous solids at finite strain. *Proc. R. Soc. London., A* (1972) **326**(1565):131–147.